

Predicted Galactic Cosmic Ray Modulation at Solar Cycle 23 Maximum

H. S. Ahluwalia

*Department of Physics and Astronomy, University of New Mexico
Albuquerque, NM 87131-1156, USA*

Abstract

We succeeded in creating the longest continuous record of the high rigidity galactic cosmic ray (GCR) intensity variations at a high latitude sea level site, spanning six solar cycles (17 to 22). Also, we reviewed the sunspot number (SSN) and the planetary index A_p data for the same time period. This led us to develop a technique for predicting the size of a SSN cycle several years in advance. In particular, we have predicted a moderate cycle 23 (more like cycle 17). A follow up of the development of cycle 23 to-date seems to bear out our prediction. In this paper we have extended Forbush's early correlation analysis of the observed long term GCR modulation. It confirms that a negative correlation continues to exist between the GCR and SSN data strings over a wide range of GCR rigidities. We have developed a methodology to predict the amplitude of GCR modulation at the maximum of cycle 23, over a range of GCR rigidity spectrum.

1 Introduction:

At the 25th ICRC, Dublin, South Africa, I reported on my success in creating the world's longest continuous record (1937-1996) of the high rigidity (ion chamber) galactic cosmic ray (GCR) intensity variations at a high latitude sea level site, spanning six solar cycles (17 to 22). We use this data string as well as two long neutron monitor (NM) data strings from Huancayo/Haleakala (1953-1998) and Climax (1951 to 1998) to extend the original Forbush (1954) analysis. We then investigate the feasibility of predicting the size of the solar cycle modulation of GCR at the sunspot number (SSN) cycle maximum.

2 Data Analysis:

The annual means for the ion chamber (IC), SSN, and the planetary index A_p are plotted in Fig. 1 for the 1937 to 1998 period (cycles 17 to 23). A_p data typically exhibit two peaks per cycle, one close to the SSN maximum and the other during the declining phase of the cycle. The former represents the amount of geomagnetic perturbation caused by the coronal mass ejections (CME) and the latter the contribution from the high speed solar wind streams (HSSWS); the latter peak is stronger. For some cycles the peaks are well separated (18, 20, 21) and for others they are very close (17, 19, 22). The minimum in A_p data typically follows that in SSN by one year. The contribution of HSSWS to GCR

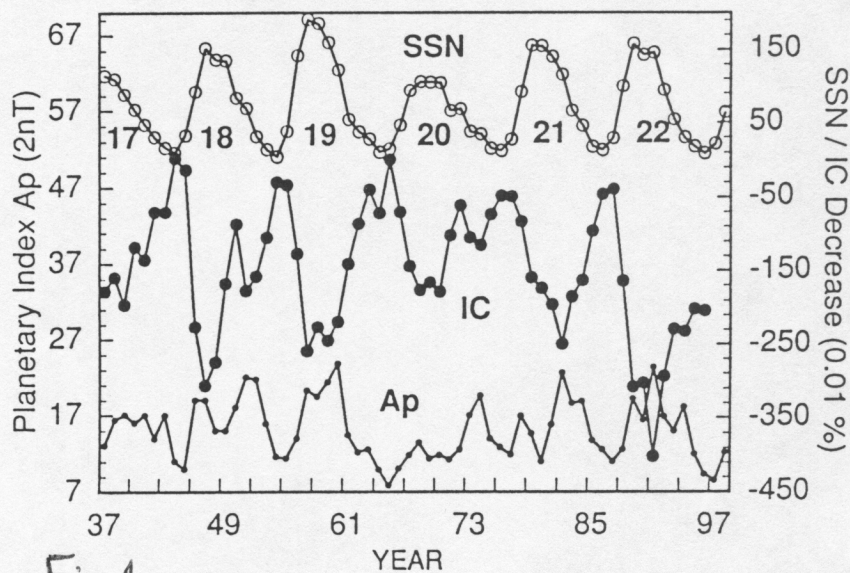


Fig.1

modulation is stronger. For some cycles the peaks are well separated (18, 20, 21) and for others they are very close (17, 19, 22). The minimum in A_p data typically follows that in SSN by one year. The contribution of HSSWS to GCR

modulation is discussed elsewhere (Ahluwalia, 1997). The inverse correlation between IC data and SSN (first pointed out by Forbush) continues to hold. For the purpose of our analysis, IC data are normalized to 100% for the year 1965; decreases from that level are plotted in Fig. 1.

3 Correlation Analysis:

The correlation between SSN and GCR data obtained with IC and two NM is depicted in Fig. 2a, b, c; NM data are normalized to 100% for May 1965. The three detectors respond to different parts of GCR differential rigidity spectrum; the median rigidity of response (R_m) for IC is 65 GV while for HU/NM, $R_m = 33$ GV and for CL/NM, $R_m = 11$ GV (Ahluwalia and Wilson, 1996). The three figures give the linear correlation between SSN and GCR at three different values of R_m . The correlation coefficients (cc) are reasonably high at the confidence level (cl) >95% although they appear to decrease as R_m increases (no explanation is available for this). The analysis therefore confirms Forbush's conclusion for a dataset extending over a much longer time period and covering different parts of the GCR spectrum. The fit parameters for the corresponding cases are given by the regression equations on the top of the figures.

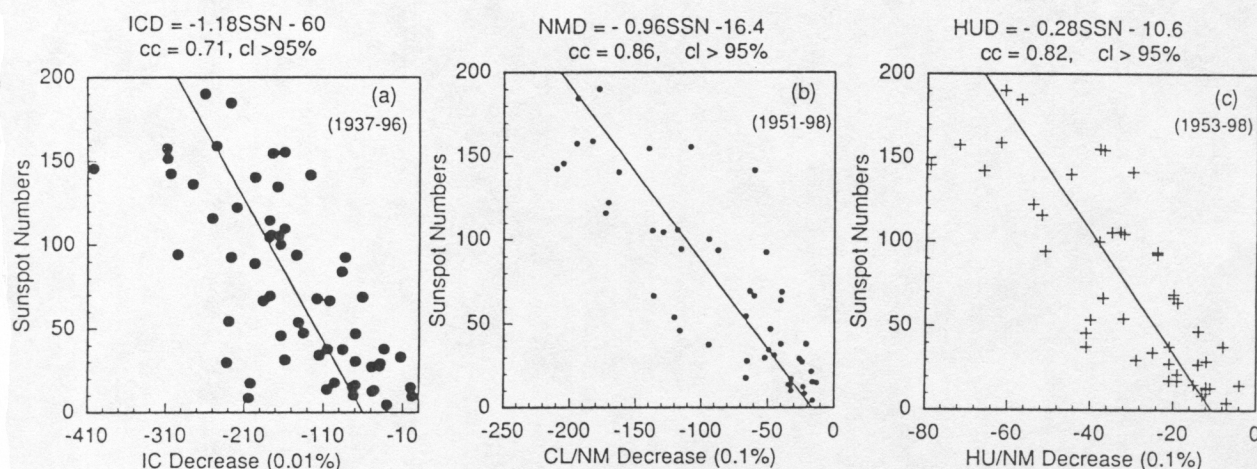


Fig. 2 a, b, c

Table 1. Solar Activity Cycle and GCR Data

Cycle	Solar Activity, SSN		GCR Data (Years)		
	Minimum (m)	Maximum (M)	IC	HU/NM	CL/NM
17	1933 (5.7)	1937 (114.4)	1	-	-
18	1944 (9.6)	1947 (151.6)	4	-	-
19	1954 (4.4)	1957 (190.2)	4	4	4
20	1964 (10.2)	1968 (105.9)	5	5	5
21	1976 (12.6)	1979 (155.4)	4	4	4
22	1986 (13.6)	1989 (157.6)	4	4	4
23	1996 (8.6)	? (131.5p)	-	3	3

SSN for m and M are in parenthesis, p is the predicted value of M for cycle 23.

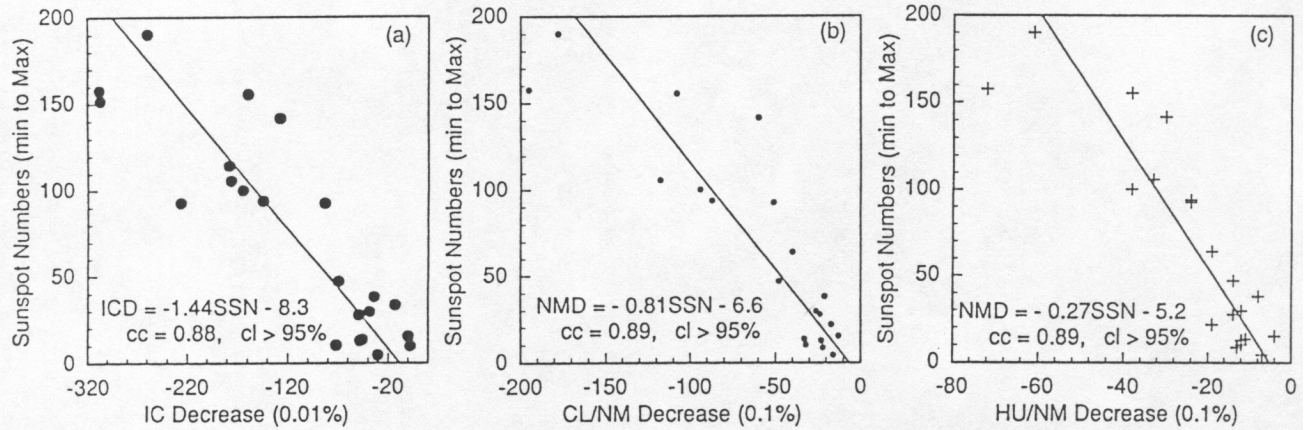


Fig. 3a, b, c

4 Ascending Phase of the Solar Cycle:

Table 1 summarizes the data pertaining to the ascending phases of the seven cycles (17 to 23) and the data from corresponding GCR detectors available to us. Annual mean SSN at the minimum (m) and maximum (M) epochs are given in the parenthesis; predicted value of SSN for cycle 23 at M is listed in the last row (Ahluwalia, 1999).

Some cycles rise to M faster (18, 19, 21, 22) than others (17 and 20). In Fig 3a, b, c, we have plotted GCR decreases against the corresponding SSN during the ascending phases of the seven cycles. In all cases, $cc = 0.9$ independent of R_m (unlike in Fig. 2) at $cl > 95\%$. So the fits are slightly more tight than in Fig. 2a, b, c. The respective regression equations for the modulated GCR intensities are summarized below.

$$\begin{aligned} \text{IC decrease (ICD)} &= -1.44 \text{ SSN} - 8.3, \quad 0.01\% \quad (1) \\ \text{HU/NM decrease} &= -0.27 \text{ SSN} - 5.2, \quad 0.1\% \quad (2) \\ \text{CL/NM decrease} &= -0.81 \text{ SSN} - 6.6, \quad 0.1\% \quad (3) \end{aligned}$$

Table 2. Observed (O) and Predicted (P) GCR Decreases at SSN Maximum

Cycle	IC (%)			HU/NM (%)			CL/NM (%)		
	O	P	P-O	O	P	P-O	O	P	P-O
17	1.8	1.7	0.1	-	-	-	-	-	-
18	3.1	2.3	0.8	-	-	-	-	-	-
19	2.6	2.8	-0.2	6.1	5.7	0.4	17.8	16.0	1.8
20	1.8	1.6	0.2	3.3	3.4	-0.1	11.8	9.2	2.6
21	1.6	2.3	-0.7	3.8	4.7	-0.9	10.8	13.3	-2.5
22	3.1	2.4	0.7	7.2	4.8	2.4	19.4	13.4	6.0
23	-	2.0p	?	-	4.1p	?	-	11.3p	?

The observed (O) and the predicted (P) GCR decreases at M are listed in Table 2. We underpredict GCR decreases for cycle 22, for all three values of R_m . Although cycle 22 had unusual characteristics (Ahluwalia, 1992, 1999, and Ahluwalia and Xue, 1993), it is not clear yet what the underlying physical cause is. This work is in progress and will be reported elsewhere. The predicted GCR modulation for cycle 23 maximum is listed in the last row.

Table 3. Rigidity Dependence of GCR Modulation

Cycle	HU/IC	CL/IC	CL/HU
19	2.35	6.85	2.92
20	1.83	6.56	3.58
21	2.38	6.75	2.84
22	2.32	6.26	2.69
23	?	?	?

In Table 3 we have listed the mean ratios of the observed GCR modulation for cycles 19 to 22. It is interesting to note that cycle 19 is the most active cycle ever, cycle 22 the second most active and cycle 21 the third most active cycle. Even so, the ratios are fairly stable in proportion to the respective values of the inverse ratios of R_m . There is almost no difference between the mean values of the ratios for the even (20, 22) and odd (19, 21) cycles. This is most interesting. It might indicate that GCR modulation caused by CME during the ascending phase of a SSN cycle varies inversely with the value of R_m , but is independent of its size. More work needs to be done to verify this inference.

5 Acknowledgements:

I am grateful to Cliff Lopate, University of Chicago, for the neutron monitor data. The maintenance of their detectors is supported by the National Science Foundation Grant ATM-9613963. The ion chamber data were kindly supplied by Germogen F. Krymsky and Galina V. Shafer, Institute of Cosmophysical Research and Aeronomy, Yakutsk, Russia.

6 References

- Ahluwalia, H. S. 1992, Planet. Space Sci., 40, 1227.
- Ahluwalia, H. S., & Xue, S. S., 1993, Geophys. Res. Lett., 20, 995.
- Ahluwalia, H. S., & Wilson, M. 1996, J. Geophys. Res., 101, 4879.
- Ahluwalia, H. S. 1997, J. Geophys. Res., 102, 24229.
- Ahluwalia, H. S. 1999, Adv. Space Res., in press.
- Forbush, S. E. 1954, J. Geophys. Res., 59, 525.